Volume 15
Number 14
21 July 2025
Pages 4039–4320

Catalysis Science & Technology

rsc.li/catalysis

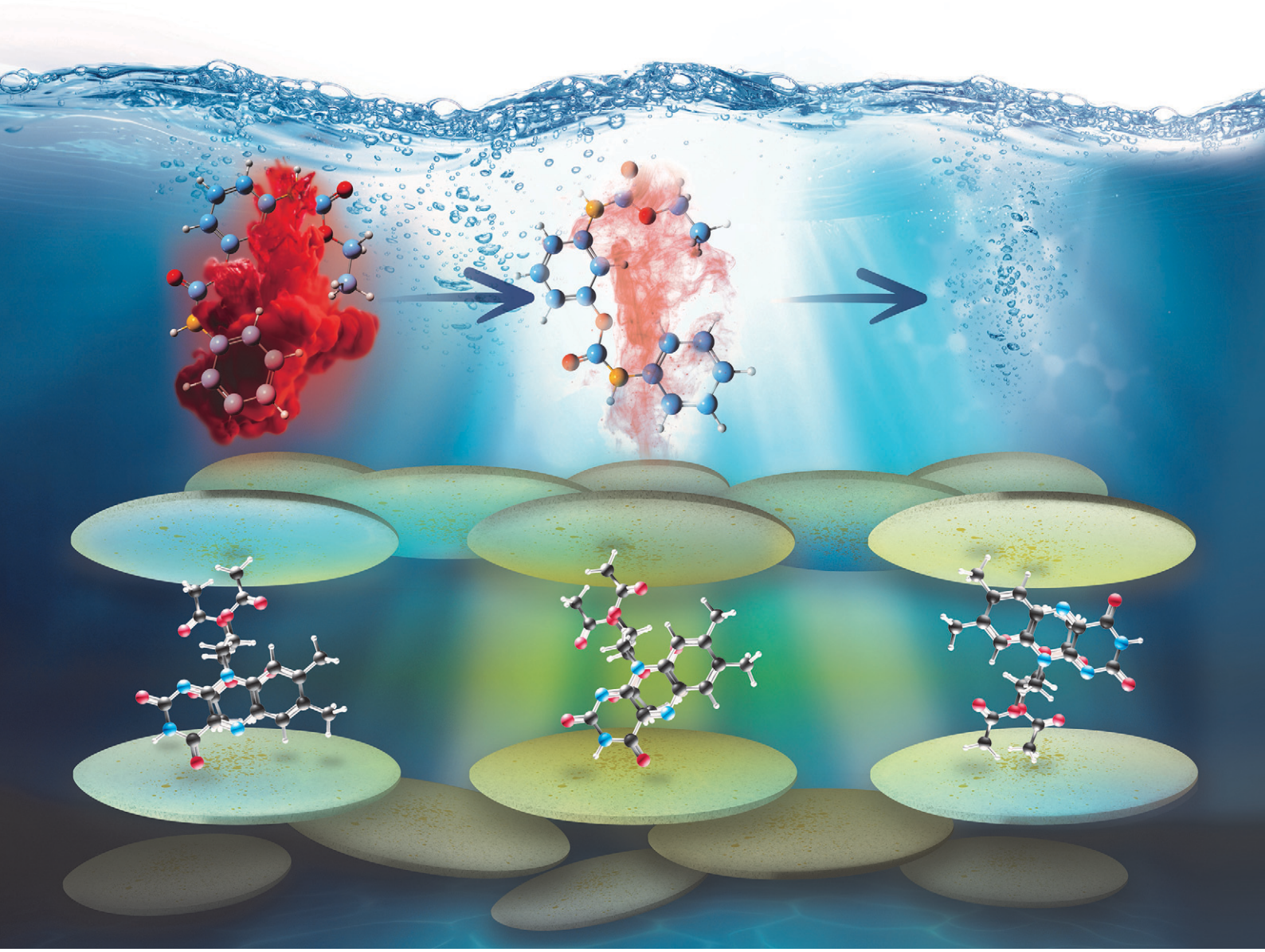

ISSN 2044-4761

ROYAL SOCIETY OF CHEMISTRY

COMMUNICATION

Ljiljana Fruk *et al.*

Flaponite: a recyclable heterogeneous flavin-based photocatalyst with LAPONITE® clay as an immobilisation scaffold

Catalysis Science & Technology

ROYAL SOCIETY OF CHEMISTRY

COMMUNICATION

View Article Online
View Journal | View Issue

Cite this: *Catal. Sci. Technol.*, 2025, **15**, 4121

Received 6th February 2025,
Accepted 26th April 2025

DOI: 10.1039/d5cy00146c

rsc.li/catalysis

Flaponite: a recyclable heterogeneous flavin-based photocatalyst with LAPONITE® clay as an immobilisation scaffold†

Anna A. Melekhova,‡[a] Matthew G. Ellis, ‡[ab] Lazina I. Zaman,[a] Ishtiaq Ahmed,[a] Alexander S. Evtushenko,[a] Thomas Kress, [c] Tijmen G. Euser [b] and Ljiljana Fruk *[a]

The low cost and biocompatible heterogeneous photocatalyst Flaponite was prepared by mixing a flavin catalytic component with LAPONITE® clay acting as a solid support. Photo-oxidation and photo-reduction of substrates under visible light irradiation were demonstrated showing that compared to flavin alone, Flaponite has enhanced photocatalytic activity and can be easily removed and recycled from the solution.

Sustainable, greener synthesis of high-value compounds aims to use less energy and fewer resources, produce less toxic waste, and employ biocompatible components, resulting in more economically and environmentally viable processes. Photocatalysis that exploits renewable solar energy is one of the most valuable strategies to achieve sustainable production of high-value compounds for the pharmaceutical industry and agricultural and energy sectors.

In the past decades, the field of photocatalysis has been dominated either by molecular photocatalysts such as ruthenium and iridium compounds, or semi-conducting (nano)structures, mostly TiO_2-based. Whereas ruthenium and iridium complexes have favorable chemical stability, long-lived excited states and strong absorption in the visible light range, they are also made of some of the rarest elements in the Earth's crust. Use of such rare metals significantly increases the cost and undermines the green value of the photocatalyst, while at the same time introducing serious environmental concerns considering their toxicity.[1] On the other hand, inorganic materials such as anatase TiO_2 are affordable and abundant and have been extensively used.[2,3] However, these materials are not as versatile in terms of their catalysed reactions and often do not absorb in the visible region, but can be tuned by addition of various dopants.[4] For example, plasmonic noble metal nanoparticles or dye sensitizers are often added to enable visible light absorption.[5] Although widely reported to be environmentally safe and non-toxic, there is a clear need to rethink the existing photocatalytic nanostructures taking into account their environmental impact and the effects of the long-term exposure.[6,7]

By large, the most sustainable, versatile, and biocompatible organic catalysts are enzymes.[8–10] Among enzymes, flavoenzymes, which contain a flavin cofactor, are involved in biological processes ranging from light sensing to metabolic tuning through the oxidation and reduction of substrates in the liver.[11,12] However, challenges of enzyme production and purification, a narrow range of optimal operating conditions (temperature and solvents) and limited recyclability often hinder their use on a large scale. While employing a flavin cofactor alone can help mitigate some of these drawbacks, the flavin moiety itself is susceptible to photodegradation and has limited solubility across a wide range of solvents. In addition, similar to flavoenzymes, flavin alone can be difficult to purify and recycle after a reaction is completed.

The issues of stability and recyclability of flavins have been addressed by the preparation of hybrid systems, which employ both inorganic and organic immobilization scaffolds. Flavins have been successfully attached to various carrier materials, including metal and metal oxide (nano) particles,[13,14] polymers[15–19] and cyclodextrins.[20–22] Such immobilization approaches resulted in improved catalytic yields, enhanced photostability, stereoselectivity and recyclability. For example, attachment of flavinium cations onto sulfated chitin enhanced their catalytic efficiency and recyclability in reactions ranging from Baeyer–Villiger oxidation to sulfoxidation, significantly improving the reaction yields of these important industrial processes.[19]

Recently, we have also shown that immobilization of flavins within organic semiconducting nanoscaffolds can

[a] *Department of Chemical Engineering and Biotechnology, University of Cambridge, Philippa Fawcett Drive, Cambridge CB3 0AS, UK. E-mail: lf389@cam.ac.uk*
[b] *Nano Photonics Centre, Cavendish Laboratory, Department of Physics, University of Cambridge, JJ Thomson Ave, Cambridge CB3 0HE, UK*
[c] *Yusuf Hamied Department of Chemistry, University of Cambridge, Lensfield Road, Cambridge, CB2 1EW, UK*

† Electronic supplementary information (ESI) available. See DOI: https://doi.org/10.1039/d5cy00146c

‡ These authors contributed equally and are considered co-first authors.

improve their stability resulting in a translatable application of the indigo dye synthesis.[17,18]

Herein, we report the design of a heterogeneous flavin-photocatalyst using a biocompatible flavin derivative, riboflavin, and a synthetic clay LAPONITE® B. LAPONITE® is an inexpensive synthetic clay extensively employed in industry, mainly as a green alternative to conventional formulation materials, in particular, in pharmaceutical and cosmetic products.[23,24] Recent studies demonstrated that it is also non-toxic to aquatic organisms, further strengthening its value as a component of green chemical product design.[25] Structurally, LAPONITE® has a layered structure and belongs to the family of 2:1 phyllosilicates. It is made of a magnesium octahedral sheet sandwiched between two silica tetrahedral sheets and sodium ions placed in the interlayer domain, with an indicative structural formula $Na_{0.7}Si_8Mg_{5.5}Li_{0.3}O_{20}(OH)_4$.[26–28] Commonly, it is represented as a clay composed of negatively charged nanodiscs with a diameter of 25 nm, 1 nm thickness, and positively charged edges.[26–28] In addition to its use for the formulation of (bio)chemical products, there has been a growing interest in LAPONITE® components for the design of heterogeneous catalysts.[29–34] Considering LAPONITE®'s low environmental footprint, biocompatibility, structural features, and availability at scale, we set out to use it as a carrier for the riboflavin moiety, which resulted in the generation of the cost-effective and efficient heterogeneous photocatalyst: Flaponite.

Flaponite was first prepared through simple mixing of a 20 mL solution of RTA (1 mM) and LAPONITE® (1 g) at 80 °C for 30 minutes, followed by drying at 120 °C for 24 hours ($Flap_{Mix}$, Fig. 1a). We also employed the lake pigment method, which has been extensively used throughout history to prevent photodegradation and prolong the shelf life of dyes.[35,36] The lake pigment method involved the addition of 400 μL of 0.5 M $KAl(SO_4)_2$ (Alum) and 700 μL of saturated $NaHCO_3$ solutions to the RTA-clay mixture before heating. Flaponite obtained by both conventional mixing ($Flap_{Mix}$) and the lake pigment method ($Flap_{LP}$) was then ground with a mortar and pestle to obtain a fine yellow powder (Fig. S1, ESI†). Characterisation by SEM and TEM revealed that there were no significant changes in the LAPONITE® morphology upon clay functionalisation, and the layered structure with disaggregated ridges of the LAPONITE® was preserved (Fig. S2–S4, ESI†). XRD analysis showed no difference in the diffraction peak patterns between the $Flap_{Mix}$ and $Flap_{LP}$ and their unmodified counterparts, LAPONITE® B and LAPONITE® LP (Fig. S5a, ESI†), while the presence of flavin was clearly indicated by the presence of three bands at 1546 cm^{-1}, 1392 cm^{-1}, and 1420 cm^{-1} in the FTIR spectra, which can be attributed to the CN and CC stretches and bends of the flavin isoalloxazine moiety (Fig. S5c and d, ESI†).[37–39] The peaks are low in intensity due to the small amount of the flavin component in Flaponite but as the ratio of flavin to LAPONITE® increases, the intensity of flavin peaks increases (Fig. S6, ESI†). In addition, ^{13}C CP/MAS NMR spectra analysis further confirmed the presence of RTA, with broadened and shifted carbon resonances in $Flap_{Mix}$ and $Flap_{LP}$ relative to neat RTA, further suggesting that flavin is adsorbed onto LAPONITE® (Fig. S7, ESI†). Considering the negatively charged facets and positively charged edges of the LAPONITE® platelets, the electron-rich flavin moiety is most likely to position itself on the sides of clay platelets through electrostatic attraction.

Both $Flap_{Mix}$ and $Flap_{LP}$ showed little signs of leakage when prepared in a solution of 50 mM EDTA, with only a 5% drop in the fluorescence intensity observed after 1 hour (Fig. S8, ESI†). This demonstrates that strong attachment is possible with and without the use of the lake pigment method, making Flaponite an ideal candidate for heterogeneous catalysis.

To explore the photocatalytic properties of Flaponite, both the photo-oxidation of 2,2′-azino-bis(3-ethylbenzothiazoline-6-sulfonic acid) (ABTS) (Fig. 1b) and the photo-reduction of amaranth (Fig. 1c) were monitored using a custom built optical setup to allow for *in situ* absorbance spectroscopy measurements to be taken (Fig. S9, ESI†). The oxidation of ABTS results in the formation of $ABTS^{+\bullet}$, a coloured product with multiple absorbance features, of which the peak at 734 nm was chosen to monitor the formation over time (Fig. 2a). The activity of both Flaponite samples ($Flap_{Mix}$ and $Flap_{LP}$) was compared to that of RTA and no-catalyst controls using an adjusted concentration to ensure a similar proportion of flavin within the reaction mixture. As shown in Fig. 2b, formation of $ABTS^{+\bullet}$ is significantly faster in the presence of $Flap_{Mix}$ or $Flap_{LP}$ compared to flavin (RTA) alone. The reaction proceeded faster in the presence of $Flap_{Mix}$ compared to $Flap_{LP}$, despite both samples containing the same initial amount of RTA. Using absorbance spectroscopy, we observed that the ratio of the 450 nm peak to 375 nm

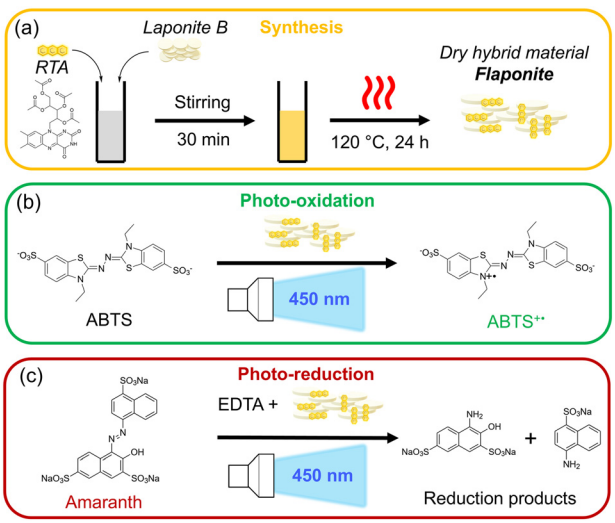

Fig. 1 (a) Preparation of the flavin-LAPONITE® hybrid (Flaponite). Illustration of the Flaponite-catalysed (b) photo-oxidation of ABTS (b) and photo-reduction of amaranth dye (c) demonstrated within this work.

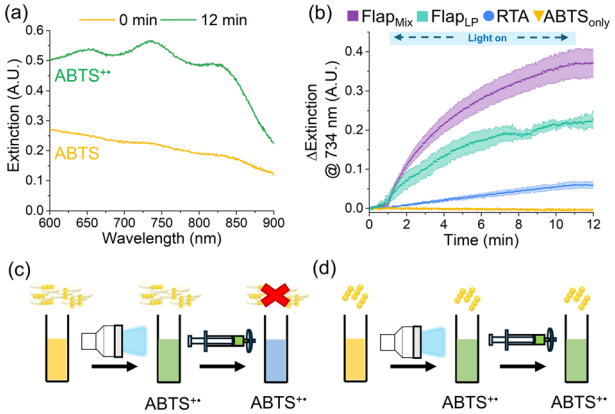

Fig. 2 (a) Extinction spectra of 2.5 mg mL^{-1} Flap$_{Mix}$ with 2.5 mM ABTS before and after light irradiation. (b) Change in extinction at 734 nm over time for Flap$_{Mix}$, Flap$_{LP}$, RTA and ABTS only (no catalyst) (n = 3). (c) Illustration of the removal of Flaponite after filtration. (d) Illustration of the lack of removal of RTA after filtration.

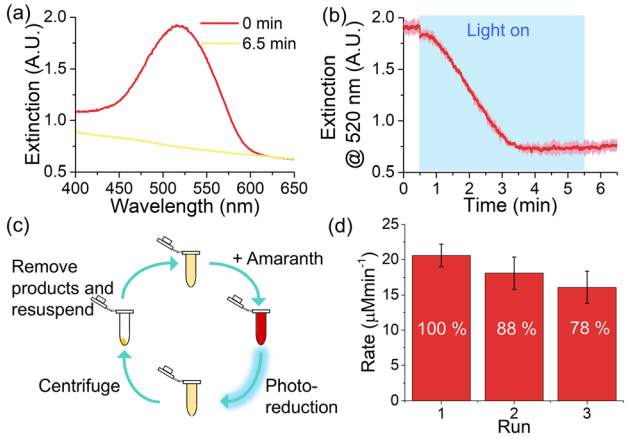

Fig. 3 (a) Extinction spectra of 0.5 mg mL^{-1} Flap$_{mix}$ and 50 μM amaranth before and after light irradiation. (b) Extinction at 520 nm over time during the photo-reduction of amaranth with Flap$_{Mix}$. (c) Scheme showing the recycling of the photocatalyst and (d) the rate of amaranth photoreduction during each sequential run (n = 3).

peak is lower for Flap$_{LP}$ compared to Flap$_{Mix}$ and RTA (Fig. S10, ESI†). This indicates that some RTA degraded to other flavin derivatives such as lumiflavin or lumichrome that would result in lower photocatalytic activity.

The reaction was also carried out using LAPONITE® alone to explore whether the clay itself facilitated the ABTS conversion. Although a steady increase in extinction over time was observed, it did not depend on irradiation and did not result in detectable color change and so is likely due to increased scatter as opposed to ABTS$^{+\bullet}$ formation (Fig. S11a and b, ESI†). The photostability of Flap$_{Mix}$ and Flap$_{LP}$ was found to be lower than that of RTA alone, suggesting that the enhancement in photoactivity is not related to enhanced photostability (Fig. S12a and b, ESI†). Instead, it is possible that LAPONITE® facilitates the adsorption of the ABTS substrate onto the surface, aiding the catalyst–substrate interaction. It is likely that ABTS photooxidation is mediated by the production of singlet oxygen from the catalyst while under light irradiation. The production of singlet oxygen was confirmed by the imidazole and *p*-nitrosodimethylaniline (RNO) assay, with RNO bleaching observed in samples containing Flap$_{Mix}$ (Fig. S13, ESI†).

A significant advantage of this heterogeneous system is that Flaponite can be removed from the reaction mixture using a 0.2 μm filter (Fig. 2c), as indicated by the colour of the solution changing from green to blue after filtration (Fig. S14, ESI†). In contrast, RTA cannot be removed from the solution due to its small size (Fig. 2d).

Next, we explored the photo-reduction by employing amaranth, a commonly used but toxic red textile dye. Photodegradation of amaranth and similar classes of dyes is of great interest for wastewater purification. Flap$_{Mix}$ was used to evaluate the anaerobic photo-reduction of amaranth with EDTA as an electron donor. Within a few minutes, the photo-reduction of amaranth dye results in a colour change from red (Fig. 3a, red line) to colourless (Fig. 3a, yellow line). After a brief delay (Fig. 3b), likely due to residual oxygen present in the mixture, the signal at 520 nm decreased rapidly, with complete photo-reduction achieved within 3 minutes. No change in absorbance was observed when the reaction was performed without Flaponite (Fig. S15, ESI†), and multiple cycles of photoreduction demonstrate Flaponite's potential to be employed as a reusable photocatalyst (Fig. 3c and d). The decrease in photoreduction after each successive run exhibited a linear trend, which was extrapolated to determine that the photoreduction rate would be reduced by 50% after 5.5 runs (Fig. S16, ESI†). Following subsequent reaction runs, the structure of Flap$_{Mix}$ showed no obvious signs of deterioration when observed under a SEM (Fig. S17, ESI†), suggesting that the decrease in photoreduction is most likely due to photodegradation of the flavin. In addition, Flaponite was shown to perform comparatively well when scaled to 100 mL (Fig. S18, ESI†).

Given that RTA alone cannot be recovered and recycled through centrifugation, this further highlights the advantages of Flaponite for photocatalytic applications. Previous efforts to utilize immobilized flavin were unsuccessful in demonstrating similar recyclability. For example, Nehme *et al.* observed that, despite the successful immobilization of flavin to iron oxide nanoparticles, significant amounts of flavin were released into the solution during the amaranth photo-reduction.[40] Therefore, the enhanced recyclability of Flaponite suggests that the flavin-LAPONITE® hybrid is superior to other alternative systems.

In conclusion, the flavin-LAPONITE® hybrid Flaponite, prepared using biocompatible and non-toxic components, is characterised by improved catalytic efficiency, versatility of catalyzed photoreactions, and recyclability. All of these make it a highly desirable system for use both in batch and flow reactors where on-demand activation and spatial control are required. Considering the pressing need for innovative but affordable catalysts, our bio-inspired system could find applications both in chemical synthesis and water purification,

and we are currently working on the most suitable use of the powdered formulation. However, our aim was not only to report the preparation of a novel photocatalyst, but also to highlight an effective route for the preparation of truly sustainable structures: exploiting enzyme cofactors and combining them with an inexpensive, nature-inspired clay carrier system already extensively used in industry.

Data availability

The data supporting this article have been included as part of the ESI.

Conflicts of interest

There are no conflicts to declare.

Acknowledgements

AAM and MGE contributed equally and should be considered co-first authors. AAM and LF would like to acknowledge the support from Leverhulme Trust (Grant RPG-2019-266). IA would like to acknowledge funding from Human Froniters Science Program (HFSP grant RGP0004/2019). MGE acknowledges funding from the EPSRC Centre for Doctoral Training in Sensor Technologies for a Healthy and Sustainable Future (EP/s023046/1). TGE acknowledges the Leverhulme Trust (grant RPG-2018-256). TEM analysis was funded by the EPSRC Underpinning Multi-User Equipment Call (EP/P030467/1). We would like to thank Prof. Stuart Clarke, from Cambridge University for generous donation of Laponite B, and both Prof Clarke and Dr. Christopher Jeans for valuable advice throughout the preparation process.

Notes and references

1 M. V. Bobo, J. J. Kuchta and A. K. Vannucci, *Org. Biomol. Chem.*, 2021, **19**, 4816–4834.
2 Q. Guo, C. Zhou, Z. Ma and X. Yang, *Adv. Mater.*, 2019, **31**, 1901997.
3 H. Wang, X. Li, X. Zhao, C. Li, X. Song, P. Zhang and P. Huo, *Chin. J. Catal.*, 2022, **43**, 178–214.
4 N. Sun, X. Si, L. He, J. Zhang and Y. Sun, *Int. J. Hydrogen Energy*, 2024, **58**, 1249–1265.
5 M. Miljevic, B. Geiseler, T. Bergfeldt, P. Bockstaller and L. Fruk, *Adv. Funct. Mater.*, 2014, **24**, 907–915.
6 M. Khan, M. S. A. Khan, K. K. Borah, Y. Goswami, K. R. Hakeem and I. Chakrabartty, *Environ. Adv.*, 2021, **6**, 100128.
7 Z. Luo, Z. Li, Z. Xie, I. M. Sokolova, L. Song, W. J. G. M. Peijnenburg, M. Hu, Y. Wang, Z. Luo, Z. Li, Z. Xie, M. Hu, Y. Wang, I. M. Sokolova, L. Song and W. J. G. M. Peijnenburg, *Small*, 2020, **16**, 2002019.
8 R. Mu, Z. Wang, M. C. Wamsley, C. N. Duke, P. H. Lii, S. E. Epley, L. C. Todd and P. J. Roberts, *Catalysts*, 2020, **10**(8), 832.
9 S. Zhang, S. Liu, Y. Sun, S. Li, J. Shi and Z. Jiang, *Chem. Soc. Rev.*, 2021, **50**, 13449–13466.
10 R. A. Sheldon, D. Brady and M. L. Bode, *Chem. Sci.*, 2020, **11**, 2587–2605.
11 S. O. Mansoorabadi, C. J. Thibodeaux and H. Liu, *J. Org. Chem.*, 2007, **72**, 6329–6342.
12 J. Drenth and M. W. Fraaije, in *Flavin-Based Catalysis*, 2021, pp. 29–65.
13 Y. Imada, M. Osaki, M. Noguchi, T. Maeda, M. Fujiki, S. Kawamorita, N. Komiya and T. Naota, *ChemCatChem*, 2015, **7**, 99–106.
14 S. I. Nehme, L. Crocker and L. Fruk, *Catalysts*, 2020, **10**(3), 324.
15 L. Crocker, P. Koehler, P. Bernhard, A. Kerbs, T. Euser and L. Fruk, *Nanoscale Horiz.*, 2019, **4**, 1318–1325.
16 L. Crocker and L. Fruk, *Front. Chem.*, 2019, **7**, 278.
17 B. J. Jordan, G. Cooke, J. F. Garety, M. A. Pollier, N. Kryvokhyzha, A. Bayir, G. Rabani and V. M. Rotello, *Chem. Commun.*, 2007, 1248–1250.
18 Y. Arakawa, R. Kawachi, Y. Tezuka, K. Minagawa and Y. Imada, *J. Polym. Sci., Part A: Polym. Chem.*, 2017, **55**, 1706–1713.
19 T. Sakai, M. Watanabe, R. Ohkado, Y. Arakawa, Y. Imada and H. Iida, *ChemSusChem*, 2019, **12**, 1640–1645.
20 V. Mojr, M. Buděšínský, R. Cibulka and T. Kraus, *Org. Biomol. Chem.*, 2011, **9**, 7318–7326.
21 V. Mojr, V. Herzig, M. Buděšínský, R. Cibulka and T. Kraus, *Chem. Commun.*, 2010, **46**, 7599–7601.
22 V. T. D'Souza, *Supramol. Chem.*, 2003, **15**, 221–229.
23 G. Kiaee, N. Dimitrakakis, S. Sharifzadeh, H.-J. Kim, R. K. Avery, K. M. Moghaddam, R. Haghniaz, E. P. Yalcintas, N. R. de Barros, S. Karamikamkar, A. Libanori, A. Khademhosseini and P. Khoshakhlagh, *Adv. Healthcare Mater.*, 2022, **11**, 2102054.
24 M. J. Rodrigo, M. J. Cardiel, J. M. Fraile, J. A. Mayoral, L. E. Pablo and E. Garcia-Martin, *Mater. Today Bio*, 2024, **24**, 100935.
25 S. N. Siddique, J. R. Khatiwada, S. Shrestha, C. Chio, X. Chen, E. Mohamedelhassan, J. Deng and W. Qin, *Water, Air, Soil Pollut.*, 2022, **233**, 1–16.
26 H. Z. Cummins, *J. Non-Cryst. Solids*, 2007, **353**, 3891–3905.
27 M. Ghadiri, H. Hau, W. Chrzanowski, H. Agus and R. Rohanizadeh, *RSC Adv.*, 2013, **3**, 20193–20201.
28 G. F. Perotti, H. S. Barud, Y. Messaddeq, S. J. L. Ribeiro and V. R. L. Constantino, *Polymer*, 2011, **52**, 157–163.
29 V. L. Mangesh, T. Perumal, S. Subramanian and S. Padmanabhan, *Energy Fuels*, 2020, **34**, 8824–8836.
30 X. Zhang, G. Dou, Z. Wang, J. Cheng, H. Wang, C. Ma and Z. Hao, *Catal. Sci. Technol.*, 2013, **3**, 2778–2785.
31 X. Zhang, G. Dou, Z. Wang, L. Li, Y. Wang, H. Wang and Z. Hao, *J. Hazard. Mater.*, 2013, **260**, 104–111.
32 E. Décsiné Gombos, D. Krakkó, G. Záray, Á. Illés, S. Dóbé and Á. Szegedi, *J. Photochem. Photobiol., A*, 2020, **387**, 112045.

33 G. R. Mahdavinia, M. Soleymani, M. Nikkhoo, S. M. F. Farnia and M. Amini, *New J. Chem.*, 2017, **41**, 3821–3828.
34 E. Aslan, *J. Photochem. Photobiol., A*, 2020, **390**, 112335.
35 K. Hunger and W. Herbst, in *Ullmann's Encyclopedia of Industrial Chemistry*, 2000.
36 D. Bomford and A. Roy, *A Closer Look - Colour*, National Gallery Company, 2009.
37 M. Unno, R. Sano, S. Masuda, T. Ono and S. Yamauchi, *J. Phys. Chem. B*, 2005, **109**, 12620–12626.
38 A. S. Eisenberg and J. P. M. Schelvis, *J. Phys. Chem. A*, 2008, **112**, 6179–6189.
39 M. Spexard, D. Immeln, C. Thöing and T. Kottke, *Vib. Spectrosc.*, 2011, **57**, 282–287.
40 S. I. Nehme, L. Crocker and L. Fruk, *Catalysts*, 2020, **10**, 324.